Supplement of Nat. Hazards Earth Syst. Sci., 26, 2111–2132, 2026
https://doi.org/10.5194/nhess-26-2111-2026-supplement

Natural Hazards and Earth System Sciences
Open Access
EGU

Supplement of

An improved empirical model for predicting postfire debris-flow volume in the western United States

Alexander N. Gorr et al.

Correspondence to: Alexander N. Gorr (agorr@usgs.gov)

Table S1: Additional fire information

Fire	Centroid Latitude	Centroid Longitude	Mean Annual Precip. (mm)[a]	Mean Annual Temp. (°C)[a]	Fire Size (km^2)
Apple	34.024895	-116.857495	733	10.9	131.0
Bush	33.758734	-111.371074	601	13.9	860.1
Buzzard	33.722812	-108.497297	580	8.7	206.1
Cameron Peak	40.605902	-105.595946	471	3.7	845.4
Carmel	36.417104	-121.654675	619	14.6	29.5
Cedar	32.93813	-116.76964	396	17.6	1,086
Coal Seam	39.568709	-107.372855	524	7.3	48.6
Cub Creek 2	48.66542	-120.163662	609	6.3	301.9
Dixie	40.2107	-121.047088	1018	8.9	3,965
El Dorado	34.093552	-116.956099	626	11.7	90.2
Farmington	40.997006	-111.87113	720	9.3	8.4
Flag	35.08463	-113.884319	407	11.7	6.0
Frye	32.717119	-109.865303	883	7.6	219.3
Grand Prix	34.200947	-117.52431	1003	13.3	205.6
Grizzly Creek	39.598596	-107.199826	540	6.9	124.3
Harvard	34.214363	-118.295978	494	17.8	4.2
Hermit's Peak	35.67513	-105.4067	534	8.6	1,425
Horseshoe 2	31.898296	-109.297553	768	11.1	914.9
Horton	33.690072	-109.319985	600	7.8	50.7
Missionary Ridge	37.367666	-107.555805	704	5.9	278.9
Monument	31.406257	-110.263289	498	16.2	122.3
Mosquito	39.022366	-120.675334	1343	14	315.1
Museum	35.262099	-111.61946	638	7.5	8.1
Old	34.191134	-117.255873	710	15.8	364.9
Pipeline	35.362787	-111.577509	478	8	107.0
Sayre	34.323723	-118.467499	518	17.6	45.4
Schultz	35.340236	-111.597928	517	7.9	56.5
Station	34.333405	-118.123267	643	15.7	669.2
Tadpole	32.95588	-108.248258	630	11.2	46.1
Telegraph	33.250961	-110.825247	604	14.4	757.8
Thomas	34.432918	-119.114304	606	15.4	1,141
Three Rivers	33.417712	-105.834773	811	7.5	25.7
Wallow	33.802682	-109.301473	607	7.2	2,281
Woodbury	33.504149	-111.181512	556	15.4	527.1

[a]Data from PRISM Climate Group (2025)

Table S2: Postfire debris-flow volumes from data-limited regions

Region	Fire	Watershed	Volume (m^3)	Deposit Latitude	Deposit Longitude
Northern California	Carmel	Carmel 1[a]	24	36.445615	-121.710146
Northern California	Carmel	Carmel 2[a]	30	36.445619	-121.709744
Northern California	Carmel	Carmel 3[a]	80	36.444445	-121.707822
Northern California	Carmel	Carmel 4[a]	150	36.443973	-121.707518
Northern California	Carmel	Carmel 5[a]	61	36.443002	-121.70692
Northern California	Carmel	Carmel 7[a]	171	36.440594	-121.705153
Northern California	Carmel	Carmel 8[a]	35	36.439575	-121.703463
Northern California	Carmel	Carmel 9[a]	38	36.439367	-121.703399
Northern California	Carmel	Carmel 10[a]	990	36.438628	-121.704248
Northern California	Carmel	Carmel 12[a]	182	36.445364	-121.711143
Northern California	Carmel	Carmel 13[a]	721	36.445167	-121.708737
Northern California	Dixie	Murphy Creek[b]	2,044	39.992102	-121.281254
Northern California	Dixie	Murphy Creek[b]	13,356	39.992102	-121.281254
Northern California	Mosquito	Oxbow[c]	16,561	39.000232	-120.736177
Utah	Farmington	Compton Bench N[d]	1,515	41.004600	-111.892556
Utah	Farmington	Compton Bench S[d]	511	41.004223	-111.891726
Utah	Farmington	Intake Basin[d]	597	41.000702	-111.878675
Washington	Cub Creek 2	Boulder Creek[c]	4,932	48.588038	-120.119389
Washington	Cub Creek 2	Butte Creek[c]	10,276	48.633015	-120.152082

[a]Data from Smith et al. (2021)

[b]Data from Thomas et al. (2023)

[c]Data from Gorr et al. (2025)

[d]Data from Gartner et al. (2008)

Table S3: Performance metrics for the final 29 models in the selection process, including R^2 and root mean square error (RMSE)

Rank	Model	R^2	RMSE
1[a]	$\ln V = 7.56 + 0.20 i30_{rr} + 0.75 \ln a + 1.11\sqrt{mh_{50}}$	0.66	1.31
2	$\ln V = 7.49 + 0.21 i30_{rr} + 0.74 \ln a + 1.04\sqrt{b_{50}}$	0.66	1.31
3	$\ln V = 7.61 + 0.18 i60_{rr} + 0.76 \ln a + 1.10\sqrt{mh_{50}}$	0.66	1.31
4	$\ln V = 7.54 + 0.18 i60_{rr} + 0.74 \ln a + 1.03\sqrt{b_{50}}$	0.66	1.32
5	$\ln V = 7.71 + 0.01 i60 + 0.76 \ln a + 1.08\sqrt{mh_{50}}$	0.66	1.32
6	$\ln V = 7.75 + 0.002 i15 + 0.76 \ln a + 1.08\sqrt{mh_{50}}$	0.66	1.32
7	$\ln V = 7.78 + 0.002 i30 + 0.76 \ln a + 1.08\sqrt{mh_{50}}$	0.66	1.32
8	$\ln V = 7.63 + 0.008 i60 + 0.75 \ln a + 1.01\sqrt{b_{50}}$	0.66	1.32
9	$\ln V = 7.67 + 0.003 i15 + 0.74 \ln a + 1.01\sqrt{b_{50}}$	0.66	1.32
10	$\ln V = 7.70 + 0.003 i30 + 0.74 \ln a + 1.01\sqrt{b_{50}}$	0.66	1.32
11	$\ln V = 7.62 + 0.20 i30_{rr} + 0.77 \ln a + 0.96\sqrt{mh_{23}}$	0.65	1.33
12	$\ln V = 7.66 + 0.17 i60_{rr} + 0.78 \ln a + 0.96\sqrt{mh_{23}}$	0.65	1.33
13	$\ln V = 7.76 + 0.007 i60 + 0.78 \ln a + 0.94\sqrt{mh_{23}}$	0.65	1.33
14	$\ln V = 7.69 + 0.007 i60 + 0.77 \ln a + 0.87\sqrt{b_{23}}$	0.65	1.33
15	$\ln V = -1.60 + 0.005 i60 + 1.15 \ln mfp + 1.53\sqrt{b_{50}}$	0.63	1.38
16	$\ln V = -1.51 + 0.001 i15 + 1.14 \ln mfp + 1.53\sqrt{b_{50}}$	0.63	1.38
17	$\ln V = -1.49 + 0.001 i30 + 1.14 \ln mfp + 1.53\sqrt{b_{50}}$	0.63	1.38
18	$\ln V = -1.92 + 0.15 i30_{rr} + 1.19 \ln mfp + 1.64\sqrt{mh_{50}}$	0.63	1.38
19	$\ln V = -1.92 + 0.12 i60_{rr} + 1.19 \ln mfp + 1.63\sqrt{mh_{50}}$	0.62	1.38
20	$\ln V = -1.89 + 0.004 i60 + 1.20 \ln mfp + 1.61\sqrt{mh_{50}}$	0.62	1.38
21	$\ln V = -1.80 + 0.0008 i15 + 1.20 \ln mfp + 1.61\sqrt{mh_{50}}$	0.62	1.38
22	$\ln V = -1.77 + 0.0004 i30 + 1.20 \ln mfp + 1.60\sqrt{mh_{50}}$	0.62	1.38
23	$\ln V = -1.47 + 0.005 i60 + 1.13 \ln mfp + 1.43\sqrt{b_{23}}$	0.62	1.39
24	$\ln V = -1.79 + 0.004 i60 + 1.19 \ln mfp + 1.50\sqrt{mh_{23}}$	0.62	1.40
25	$\ln V = -1.70 + 0.0007 i15 + 1.18 \ln mfp + 1.50\sqrt{mh_{23}}$	0.61	1.40
26	$\ln V = -1.67 + 0.0003 i30 + 1.18 \ln mfp + 1.50\sqrt{mh_{23}}$	0.61	1.40
27	$\ln V = 5.40 + 0.40 i30_{rr} - 1.29 \ln M_R + 2.18\sqrt{b_{50}}$	0.60	1.42
28	$\ln V = 5.46 + 0.41 i30_{rr} - 1.41 \ln M_R + 2.34\sqrt{mh_{50}}$	0.60	1.43

29	$\ln V = 5.47 + 0.35i60_{rr} - 1.26 \ln M_R + 2.20\sqrt{b_{50}}$	0.60	1.43

[a]Selected model

Table S4: Definitions of variables used by the final 29 models

Variable	Definition
a	Watershed area (km^2)
b_{23}	Watershed area burned with slopes ≥ 23° (km^2)
b_{50}	Watershed area burned with slopes ≥ 50% (km^2)
$i15$	Peak 15-minute rainfall intensity (mm/h)
$i30$	Peak 30-minute rainfall intensity (mm/h)
$i60$	Peak 60-minute rainfall intensity (mm/h)
$i30_{rr}$	i30 rainfall ratio
$i60_{rr}$	i60 rainfall ratio
mfp	Maximum flow path (m)
mh_{23}	Watershed area burned at moderate or high severity with slopes ≥ 23° (km^2)
mh_{50}	Watershed area burned at moderate or high severity with slopes ≥ 50% (km^2)
M_R	Melton ratio (ruggedness)
V	Debris-flow volume (m^3)

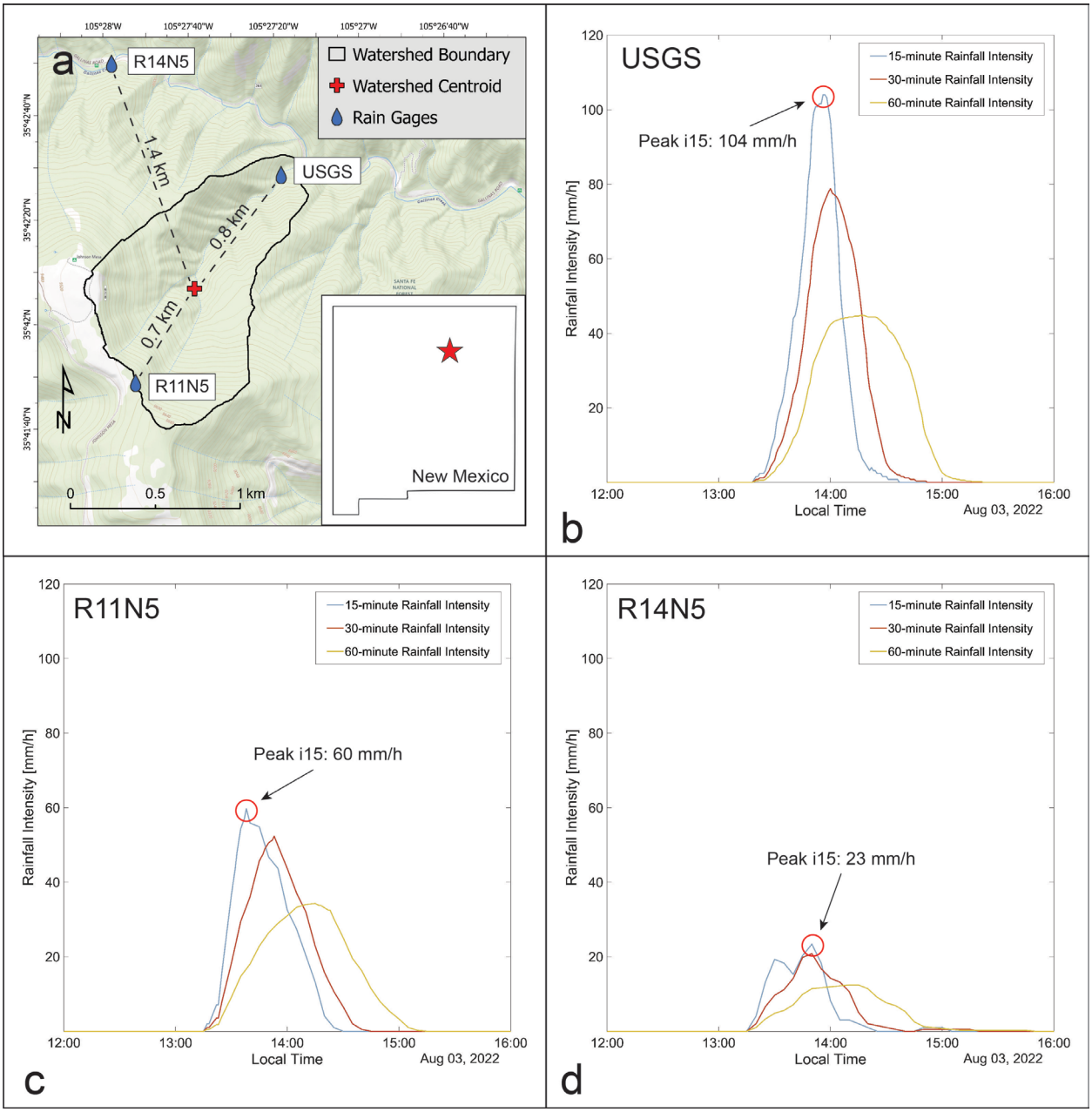

Figure S1: Rainfall data from a 2022 debris-flow-producing storm, recorded by three separate rain gages located in close proximity to one another in northern New Mexico, USA. (a) The locations of three rain gages (USGS, R11N5, and R14N5) in relation to a debris-flow-producing watershed. (b) The USGS gage, located near the watershed outlet, recorded the highest 15-minute peak rainfall intensity (i15). (c) The R11N5 rain gage, located at the drainage divide, recorded an i15 of 60 mm/h, roughly half as intense as the rainfall measured at the USGS gage. (d) The lowest rainfall intensity was measured at the R145 gage, located 1.4 km from the watershed centroid. The i15 recorded here was substantially lower than the rainfall intensities measured at either the USGS or R11N5 gages. Basemap credits: United States Geological Survey (USGS) The National Map: National Boundaries Dataset, 3D Elevation Program, Geographic Names Information System, National

Hydrography Dataset, National Land Cover Database, National Structures Dataset, and National Transportation Dataset; USGS Global Ecosystems; U.S. Census Bureau TIGER/Line data, United States Forest Service Road data; Natural Earth Data; U.S. Department of State HIU; National Oceanic and Atmospheric Administration National Centers for Environmental Information.

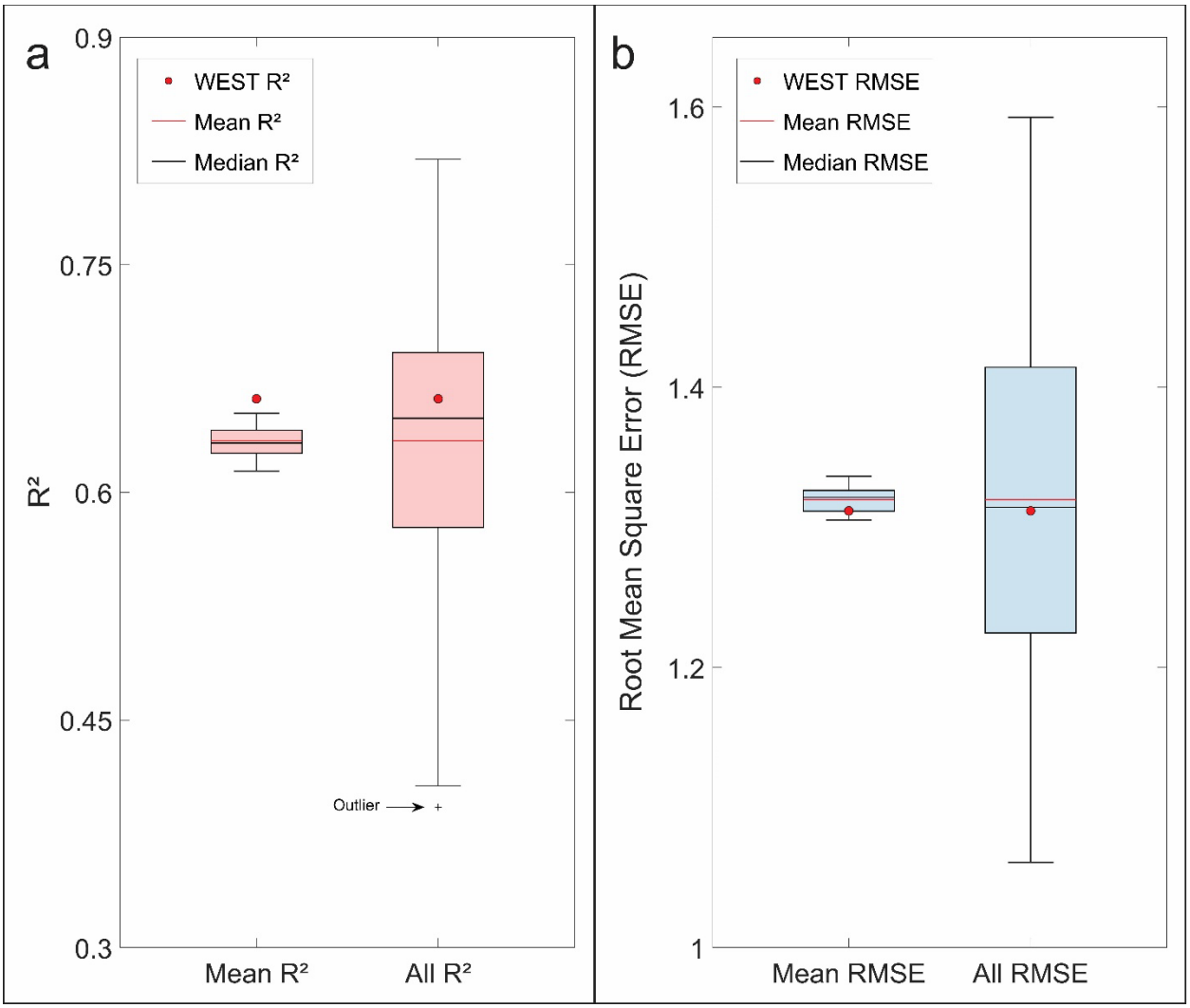

Figure S2: Box plots showing the distribution of (a) R^2 and (b) root mean square error (RMSE) values associated with the cross-validation analysis. The Mean R^2 and RMSE box plots show the distribution of the 20 mean values of these metrics, one for each of 20 iterations of fivefold cross validation. The All R^2 and RMSE box plots show the distribution of all 100 values of these metrics calculated as part of this analysis, one for all 100 folds associated with 20 iterations of fivefold cross validation. The R^2 and RMSE values associated with the final western United States (WEST) model that was trained on the entire volume database are plotted for comparison.

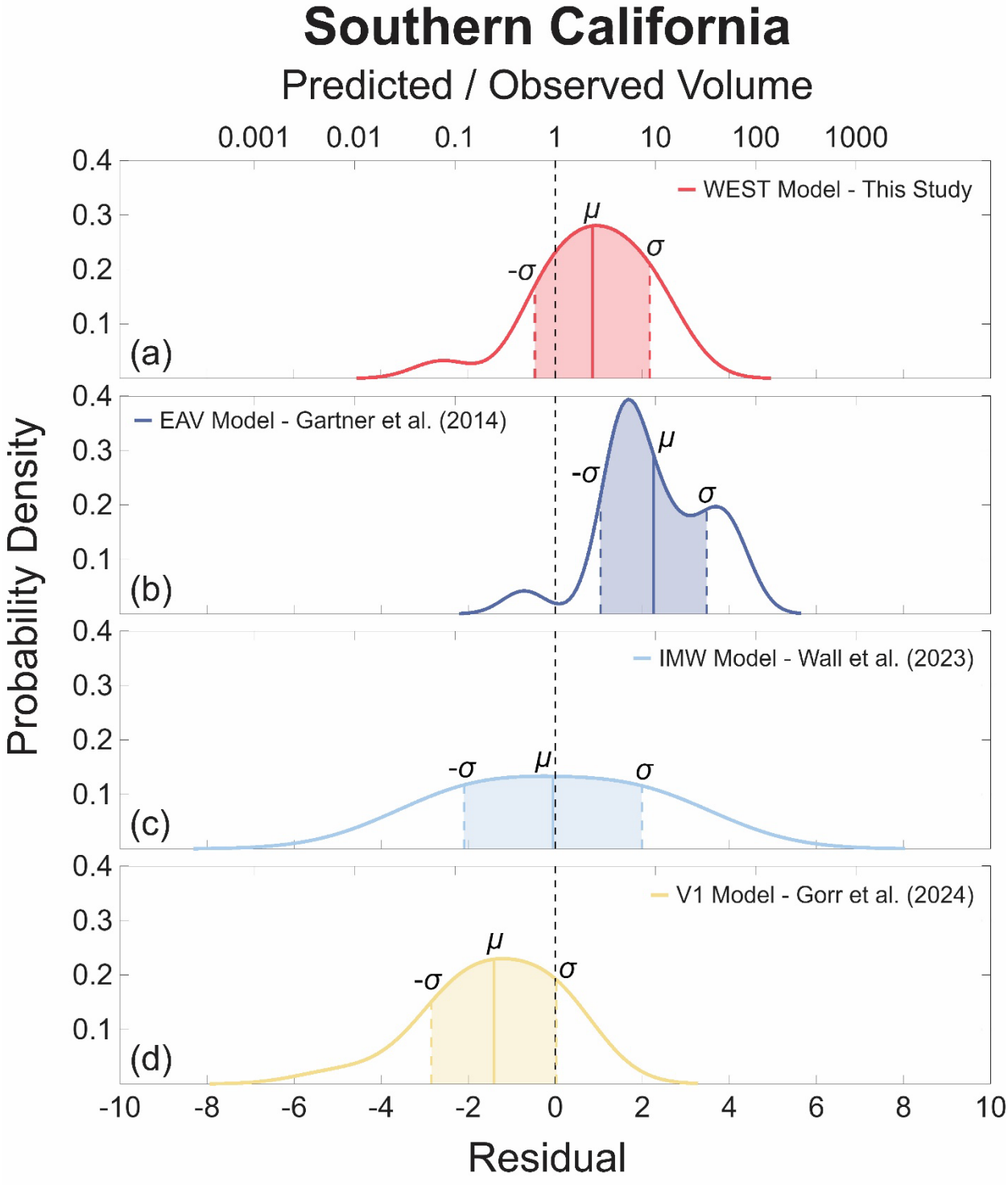

Figure S3: Probability density functions for the residuals of the (a) western United States (WEST), (b) Emergency Assessment volume (EAV), (c) Intermountain West (IMW), and (d) V1 models when applied to volume data from southern California.

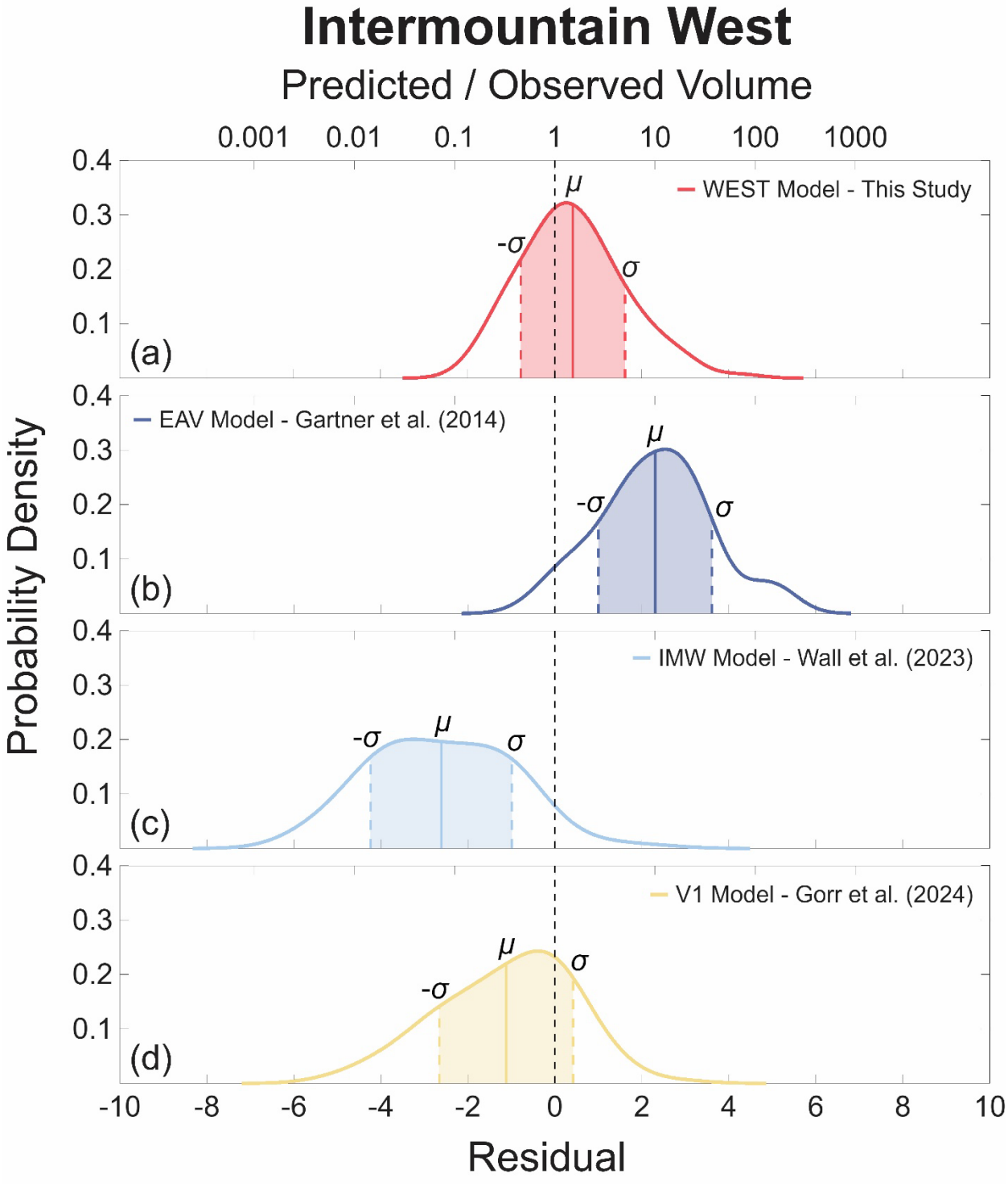

Figure S4: Probability density functions for the residuals of the (a) western United States (WEST), (b) Emergency Assessment volume (EAV), (c) Intermountain West (IMW), and (d) V1 models when applied to volume data from the Intermountain West.

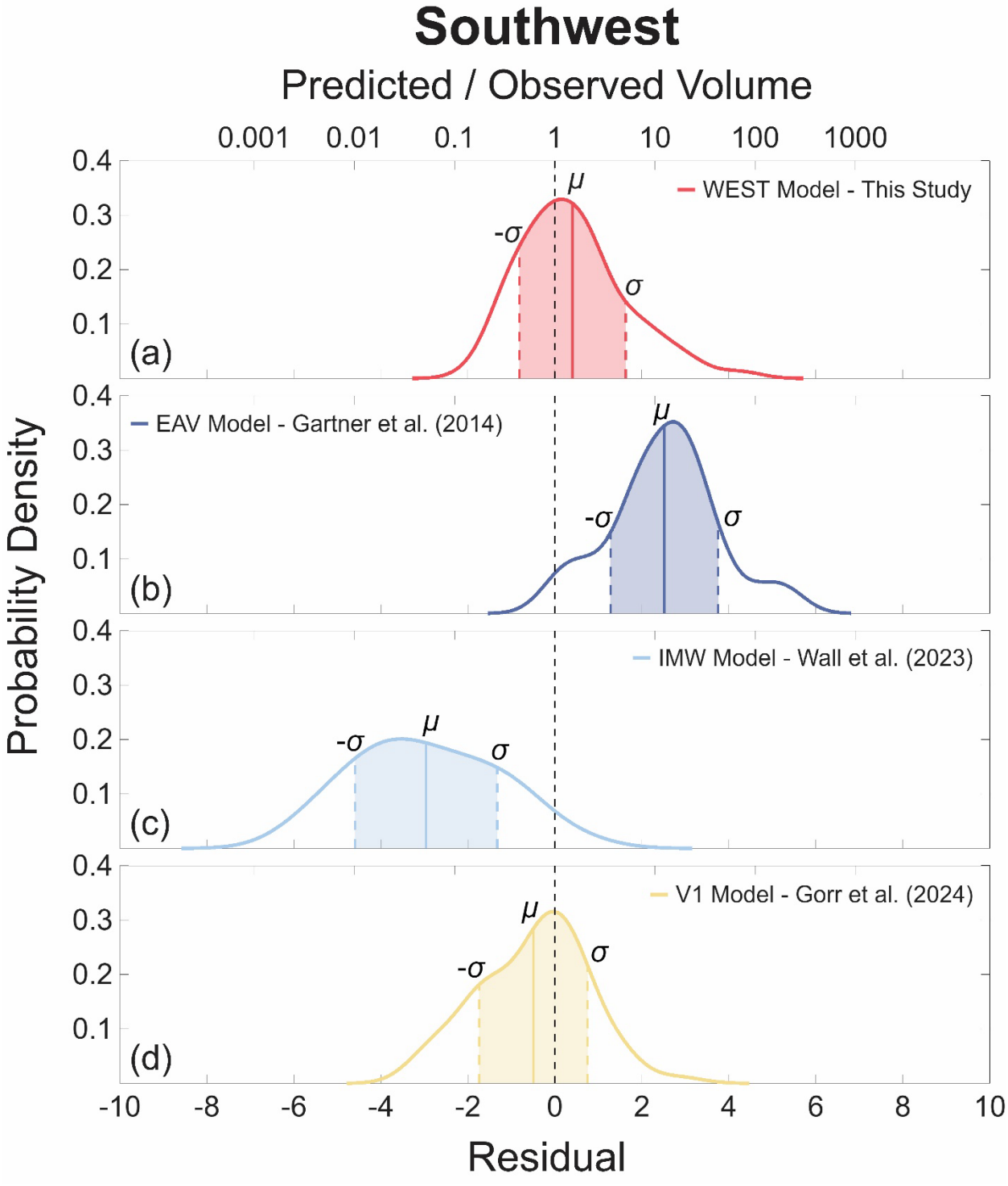

Figure S5: Probability density functions for the residuals of the (a) western United States (WEST), (b) Emergency Assessment volume (EAV), (c) Intermountain West (IMW), and (d) V1 models when applied to volume data from the Southwest.